Conformational Study of Benzene-Fused Ring Compound 1,2,3,4-Tetrahydronaphthalene Using Vibrational Laser Spectroscopy

Jaebum Choo*, Seong Jun Han†, and Young Sik Choi‡

**Department of Chemistry, Hanyang University, Ansan 425-791, Korea*
†*C & C Research Labs., 146-141 Hwasung-gun, Kyunggi-do 445-970, Korea*
‡*Department of Chemistry, Inha University, Incheon 402-751, Korea*
Received May 22, 1997

The infrared, Raman, and jet-cooled laser-induced fluorescence excitation spectra of 1,2,3,4-tetrahydronaphthalene have been recorded and analyzed. The observed vibrations have been assigned to understand the conformational behaviors in its electronic ground (S_0) and excited (S_1) states. *Ab initio* at the HF/6-31G** level and molecular mechanics (MM3) force field calculations have been carried out to generate the complete normal mode frequencies of the molecule in its S_0 state. The vibrational frequencies calculated from the *ab initio* method show a better agreement with the observed infrared and Raman frequencies than those calculated from the MM3 method. In several cases, the normal mode calculations were very helpful to clarify some ambiguities of previous assignments. In addition, the ring inversion process between two twisted conformers of 1, 2,3,4-tetrahydronaphthalene has been reexamined utilizing *ab initio* calculation. The results show that the ring inversion energy is in the range of 3.7-4.3 kcal/mol which is higher than the previously reported AM1 value of 2.1 kcal/mol.

Introduction

Vibrational spectroscopy, such as infrared or Raman, has served as a powerful tool for studying the conformations and dynamics of small ring molecules in their electronic ground states (S_0).[1] Recently, the research area for the conformational studies of ring systems has been extended to the electronic excited state (S_1) with the development of pump-probe vibrational methods and supersonic jet techniques. Benzene-fused bicyclic ring molecule has been one of the good target molecules because the structure and dynamics of this molecule, in its $\pi \rightarrow \pi^*$ excited singlet state, can be investigated using jet-cooled laser-induced fluorescence excitation spectroscopy. Several spectroscopic investigations of the excited state of benzene-fused rings have been reported using this technique.[2]

Recently, Chowdhury *et al.* have investigated the jet-cooled fluorescence excitation and the single vibronic level luminescence spectra of 1,2,3,4-tetrahydronaphthalene (tetralin) to understand the conformational change in its S_0 and S_1 states.[3] However, only a few vibrational descriptions in the low frequency region have been reported and a detailed analysis of spectroscopic data has not been attempted. In the present paper, therefore, we report the infrared and Raman spectra of tetralin and its complete vibrational assignments based on group frequency considerations and Raman depolarization ratios.[4] Frequency calculations using the *ab initio* and MM3 methods have been carried out for the accurate assignments of observed spectral bands and the proper analyses of such spectra. In addition, the supersonic jet-cooled laser-induced fluorescence (LIF) excitation spectrum of tetralin has been recorded and analyzed to understand the conformational dynamics of its S_1 state. The LIF spectrum was analyzed by comparing it with the S_0 frequencies as well as the previous assignments of 1,4-benzodioxan, where a benzene ring is fused to a two-oxygen containing saturated six-membered ring.[5]

The ring inversion process of cyclohexene has been extensively investigated by spectroscopic and computational methods, and the barrier for this process was estimated to be in the 8.4-12.1 kcal/mol range.[6] The ring inversion process of tetralin, where a benzene ring is fused to a six-membered ring, is very similar to that of cyclohexene. That is, the lowest energy conformation of tetralin is a half chair (twisted) conformation (C_2) and the molecule can interconvert one twisted form to another through the bending form (C_s).

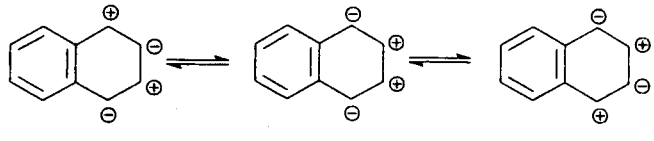

Chowdhury and co-workers examined the conformational change of tetralin using semi-empirical AM1 calculation and predicted the inversion barrier to be 2.1 kcal/mol.[3] This value is, however, too low compared with the value of cyclohexene even though we considered the fact that the rigidity of a benzene ring reduces the inversion potential of tetralin. Thus, we reexamined the inversion process of tetralin using *ab initio* and molecular mechanics (MM3) calculations to determine a more accurate inversion barrier. The calculated potential profiles show that the ring inversion barrier is in fact much higher than that determined from the AM1 calculation. In the present paper, an origin for this discrepancy will be discussed.

*To whom correspondence should be addressed.

Experimental

The mid- and far-infrared spectra were recorded on a Bio-Rad FTS-6000 interferometer operating at a resolution of 1.0 cm^{-1}. A cryogenic MCT detector and KBr windows were used for the mid-infrared measurements. On the other hand, a DTGS detector and a 2.0 mm wavelength polyethylene cell were used for the far-infrared measurements.

The Raman spectra were recorded on an ISA Jobin Yvon U-1000 monochromator equipped with a Coherent Radiation Innova 20 argon ion laser source. The laser line at 514.5 nm was used as the excitation source and a spectral resolution between 1 and 2 cm^{-1} were employed. A rotatable polarizer was used to measure the depolarization ratios of the Raman bands.

The LIF experimental apparatus for the tunable Nd:YAG dye laser and supersonic jet cooling system has been previously described.[7] The frequency-doubled output of a Nd:YAG pumped dye laser (Spectra Physics GCR-150) was used as the excitation source. The laser beam was focused onto the expanding supersonic jet stream which was expanded through a nozzle with a 0.5 mm diameter. Helium served as the carrier gas, typically with a backing pressure of 600 torr. Fluorescence from the excited molecules was collected with a quartz lens, filtered with a color filter, and then detected with a PMT (Hamamastu H1161). Frequency calibration of the system was accomplished by recording the optogalvanic spectrum of a Ne hollow cathode lamp. The frequencies reported here are accurate to ± 0.3 cm^{-1}.

1,2,3,4-Tetrahydronaphthalene was purchased from Aldrich Chemical Co., and used without further purification.

Computations

The *ab initio* calculations were carried out using the Gaussian 94 program package[8] on a CRAY C-90 supercomputer. The calculations were performed at the HF/6-31G** basis set level. A full geometry optimization was performed to find the minimum energy and equilibrium structure of the molecule and then the calculations of harmonic force constants and normal modes in Cartesian coordinates were followed. The optimum geometry was confirmed by the vibrational frequency calculations. A scaling factor of 0.89 was used in comparing the *ab initio* calculated frequencies with the observed frequencies. The potential energy profile for the ring inversion process was obtained by increasing the CH_2-CH_2-CH_2-CH_2 torsional angle from a twisted conformation (τ=64°) to a bent conformation (τ=0°). Molecular mechanics calculations were carried out using the MM3 program.[9]

Results and Discussion

Vibrational Analysis of Tetralin in its S_0 State

The *ab initio* and MM3 calculations demonstrate that the equilibrium structure of tetralin is a non-planar twisted form. (C_2 symmetry) The sixty vibrations of tetralin, under the C_2 point group, belong to the irreducible representation 31A+29B. Selection rule permits all the vibrational modes to be infrared and Raman active.

Figures 1 and 2 show the liquid-phase infrared spectra of tetralin in the 600-3300 and 80-650 cm^{-1} regions, respectively. These figures also show the vibrational bands calculated from the *ab initio* method at the HF/6-31G** basis set level. As shown in the figures, the calculated infrared frequencies and intensities are very consistent with the observed values. The quality of the far-infrared spectrum is somewhat poorer than the mid-infrared one, due to the weak intensity of the infrared signal in the far-infrared region as well as a strong coupling among the low-frequency fundamental bands. The ambiguous spectral bands in the far-infrared region, however, could be accurately assigned based on the *ab initio* frequency calculations. Figures 3 and 4 show the liquid-phase Raman spectra, measured with parallel and perpendicular polarizations. The depolarization ratio for each Raman line can be used to assign different spectral lines to different vibrations by comparing the experimental results with those predicted by group theory. Most of the Raman lines for totally symmetric vibrations (species A) have been strongly polarized, whereas the Raman lines for

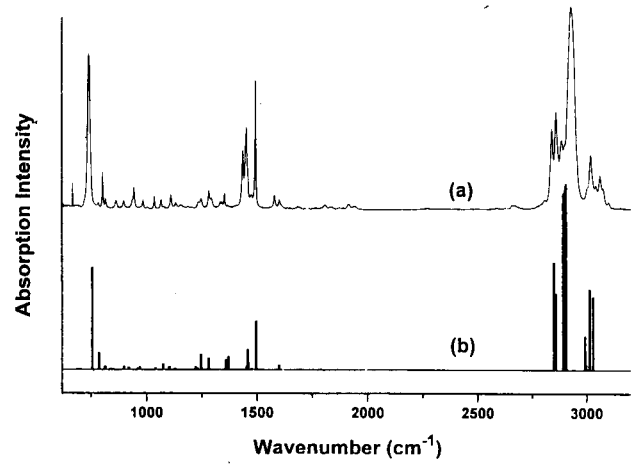

Figure 1. Observed and calculated infrared spectra of tetralin in the 600-3300 cm^{-1} region: (a) liquid-phase mid-infrared spectrum; (b) calculated mid-infrared spectrum from the *ab initio* (HF/6-31G**) method.

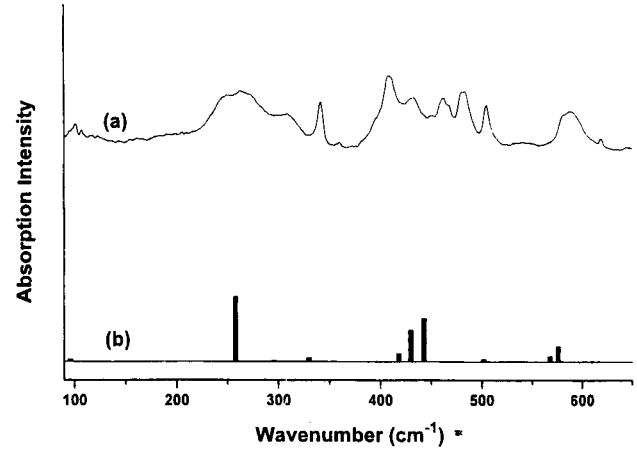

Figure 2. Observed and calculated infrared spectra of tetralin in the 80-650 cm^{-1} region: (a) liquid-phase far-infrared spectrum; (b) calculated far-infrared spectrum from the *ab initio* (HF/6-31G**) method.

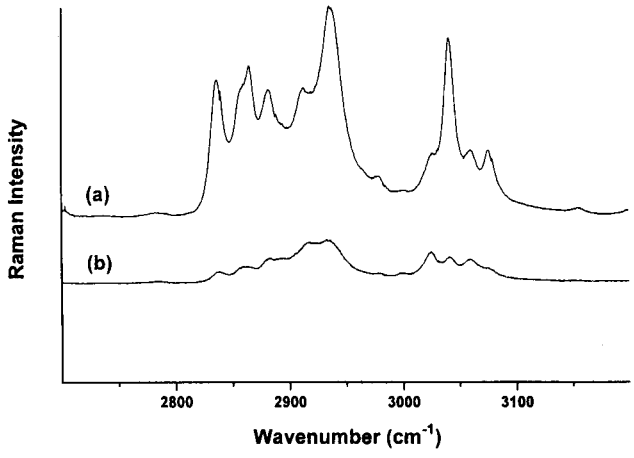

Figure 3. Liquid-phase Raman spectra of tetralin in the 2700-3200 cm^{-1} region: (a) polarized; (b) depolarized.

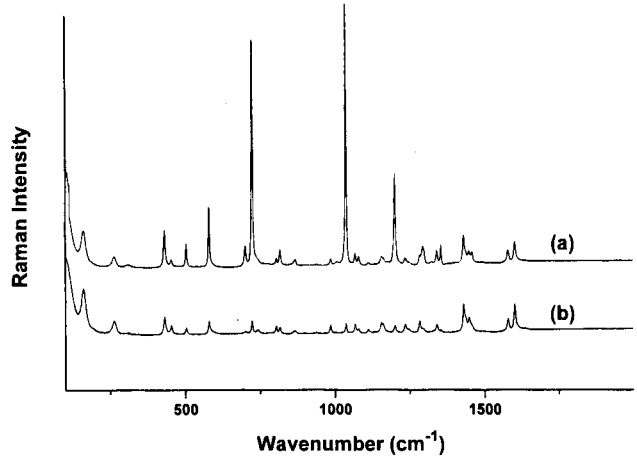

Figure 4. Liquid-phase Raman spectra of tetralin in the 100-2000 cm^{-1} region: (a) polarized; (b) depolarized.

asymmetric vibrations (species B) have been depolarized.

Table 1 shows the assignments of the observed (infrared and Raman) and the calculated (*ab initio* and MM3) fundamental vibrational frequencies for tetralin. As shown in the table, the frequencies calculated from the *ab initio* method show a better agreement with the observed infrared and Raman frequencies than those calculated from the MM3 program. However, the calculated *ab initio* frequencies, for C-H stretching vibrations in the 2800-3100 cm^{-1} region, disagree with the observed values. Pulay reported that the harmonic force constants and frequencies calculated from the *ab initio* method usually overestimate the corresponding experimental values because anharmonicity lowers the frequencies.[10] The overestimation of the frequencies can be corrected by multiplying an empirical scaling factor 0.89 to the calculated values. The disagreement of the C-H stretching bands, however, in the 2800-3100 cm^{-1} region suggests that the anharmonicity corrections of the fundamental frequencies for the C-H stretching modes are less accurate than those of the lower frequency modes. Recently, density functional theory (DFT) is widely used to calculate more accurate vibrational frequencies for aromatic compounds.[11] The frequency calculation using the DFT technique is in progress and the results are expected to improve the force field errors of the Hartree-Fock theory in the C-H stretching region. Table 1 also presents the low frequency assignments previously reported by Chowdhury and co-workers.[3]

C-H stretching region (2800-3100 cm^{-1}). Two symmetric and antisymmetric vibrational modes, for =CH stretching motions of a benzene ring, belong to A and B symmetry, respectively. The corresponding vibrational bands were observed in the range 3000-3100 cm^{-1}. Eight vibrational modes, for $-CH_2$ stretching motions of an unsaturated six-membered ring, were observed in the range 2830-3000 cm^{-1}. Although the fundamental C-H stretching modes were coupled together, they could be accurately assigned based on the Raman depolarization ratios and the force field frequency calculations. All the Raman lines for the C-H stretching modes in A block were strongly polarized, whereas the six Raman lines in B block were depolarized. The vibrational frequencies calculated from the MM3 program were more consistent with the observed frequencies than the values calculated from the *ab initio* method in this region. The deviation of 40-60 cm^{-1} between the *ab initio* and observed frequencies, for the C-H stretching motions, was caused by the incorrect anharmonic force field correction of the Hartree-Fock theory, and this inconsistency is expected to be improved by applying the selective scaling factors or the density functional methods.

Finger print region (700-1600 cm^{-1}). The benzene ring stretching modes were observed in the range 1400-1600 cm^{-1}. The infrared intensities were relatively stronger than those of the Raman lines for these vibrational modes. The $-CH_2$ deformation, wag and twist modes in A and B symmetry blocks were observed in the range 1100-1450 cm^{-1}. The Raman lines at 1354 and 1202 cm^{-1} were strongly polarized. The weak Raman lines and infrared bands in the 1000-1300 cm^{-1} region were assigned to the in-plane and the out-of-plane =CH wag modes, respectively. The three bands in the 800-950 cm^{-1} range were assigned to $-CH_2$ rock modes. The five ring stretching modes, for the saturated six-membered ring, in A and B symmetry blocks were observed in the range 700-1100 cm^{-1}. All the observed vibrational bands in this region were assigned based on the frequencies calculated from the *ab initio* and MM3 methods and they coincided very well.

Low frequency region (100-700 cm^{-1}). The four fundamental bands (ν_{29}, ν_{55}, ν_{58}, and ν_{60}), which were not observed in the Raman spectrum, could be identified in the infrared spectrum. All the fundamental assignments, except the ν_{57} mode, were consistent with the previous assignments by Chowdhury *et al.*[3] The vibrational band at 431 cm^{-1} had been previously assigned to a second overtone from the single vibronic level luminescence (SVL) spectra. This band, however, was reassigned to the fundamental mode for the ring angle deformation based on the force field calculation. The lowest frequency vibration, the ring puckering, was observed at 101 cm^{-1} in the far-infrared spectrum and the corresponding calculated frequency was 96 cm^{-1}. The next lowest frequency vibration, the saturated six-membered ring twisting, was observed at 161 cm^{-1} in the Raman spectrum.

These assignments provide a reasonable picture of the vibrational structure of the molecule and the *ab initio* calculation at the HF/6-31G** level supports the needed in-

Table 1. Observed and calculated fundamental vibrational frequencies (cm^{-1}) of tetralin

	Raman	Infrared	HF/6-31G**	MM3	Chowdhury *et al.*[a]
A					
ν_1 =CH sym. stretch	3074 P	3075	3028	3055	–
ν_2 =CH sym. stretch	3041 P	3041	2996	3041	–
ν_3 -CH_2 sym. stretch	2937 P	2928	2899	2947	–
ν_4 -CH_2 sym. stretch	2912 P	–	2893	2946	–
ν_5 -CH_2 anti-sym. stretch	–	2896	2855	2904	–
ν_6 -CH_2 anti-sym. stretch	2860	–	2849	2891	–
ν_7 Benzene ring stretch	1580	1579	1600	1673	–
ν_8 Benzene ring stretch	1498	1493	1496	1575	–
ν_9 Benzene ring stretch	–	1473	1475	1574	–
ν_{10} Benzene ring stretch	1448	1451	1448	1462	–
ν_{11} -CH_2 deformation	–	–	1370	1460	–
ν_{12} -CH_2 deformation	1354 P	1353	1358	1427	–
ν_{13} -CH_2 wag	–	1248	1247	1396	–
ν_{14} -CH_2 wag	1202 P	1201	1222	1238	–
ν_{15} -CH_2 twist	–	1189	1188	1226	–
ν_{16} -CH_2 twist	1154	1154	1155	1196	–
ν_{17} =CH out-of-plane wag	–	–	1088	1177	–
ν_{18} =CH out-of-plane wag	1079	1078	1075	986	–
ν_{19} =CH in-plane wag	1068	1066	1040	1078	–
ν_{20} Ring stretch	1036 P	1037	1016	1039	1046
ν_{21} =CH in-plane wag	1005	1003	1003	1004	–
ν_{22} Ring stretch	886	–	887	986	867
ν_{23} -CH_2 rock	–	–	837	855	–
ν_{24} -CH_2 rock	817	816	813	835	–
ν_{25} Ring stretch	724 P	698	713	783	725
ν_{26} Benzene ring twist	700	–	695	697	702
ν_{27} Ring angle deformation	580 P	587	568	604	581
ν_{28} Benzene ring twist	504 P	505	502	555	505
ν_{29} Ring angle deformation	–	409	418	384	–
ν_{30} Double bond torsion	310	306	296	309	310
ν_{31} Saturated ring twist	161	–	144	140	160
B					
ν_{32} =CH anti-sym. stretch	3059	3059	3012	3049	–
ν_{33} =CH anti-sym. stretch	3026	3016	2991	3039	–
ν_{34} -CH_2 sym. stretch	2980	3000	2904	2949	–
ν_{35} -CH_2 sym. stretch	2882	2882	2891	2944	–
ν_{36} -CH_2 anti-sym. stretch	2865	2858	2857	2899	–
ν_{37} -CH_2 anti-sym. stretch	2836	2838	2848	2885	–
ν_{38} Benzene ring stretch	1603	1601	1630	1693	–
ν_{39} -CH_2 deformation	1459	–	1461	1517	–
ν_{40} -CH_2 deformation	1448	–	1457	1451	–
ν_{41} Benzene ring stretch	1429	–	1435	1424	–
ν_{42} =CH in-plane wag	–	1363	1359	1410	–
ν_{43} =CH in-plane wag	1341	1340	1341	1350	–
ν_{44} -CH_2 wag	1284	1283	1281	1257	–
ν_{45} -CH_2 wag	1235	1235	1231	1222	–
ν_{46} -CH_2 twist	1161	1189	1165	1197	–
ν_{47} -CH_2 twist	–	1134	1129	1188	–
ν_{48} Ring stretch	1111	1111	1103	1071	–
ν_{49} Ring stretch	945	939	959	962	–
ν_{50} -CH_2 rock	939	945	921	881	–
ν_{51} -CH_2 rock	900	899	899	847	–
ν_{52} Ring angle deformation	–	898	899	837	–
ν_{53} =CH out-of-plane wag	743	–	786	793	–
ν_{54} =CH out-of-plane wag	741	741	756	647	–
ν_{55} Ring angle deformation	–	585	576	558	–
ν_{56} Benzene ring puckering	454	463	443	443	454
ν_{57} Ring angle deformation	431	433	430	374	$3\nu_{31}$*
ν_{58} Ring angle deformation	–	342	331	328	–
ν_{59} Ring flapping	264	261	258	240	265
ν_{60} Ring puckering	–	101	96	96	105

P=polarized. [a] Reference 3. *Frequency has been reassigned.

formation for clarification of the vibrational assignments.

Vibrational Analysis of Tetralin in its S_1 State

The jet-cooled fluorescence excitation spectrum has been recorded and analyzed to understand the vibrational structure of tetralin in its S_1 electronic excited states. Figure 5 shows the low-frequency fluorescence excitation spectrum of tetralin which has been recorded in the 265-273 nm region and the vibrational assignments are summarized in Table 2. We basically agree with Chowdhury's assignments[3] for ν_{31}, ν_{30}, ν_{28}, ν_{26}, and ν_{25} but we disagree with the assignments for ν_{59} and ν_{39}. In addition, a couple of fundamental bands and four combination bands were observed in our spectrum. The strongest band in the spectrum occurred at 36788.4 cm^{-1} and this band was assigned as the electronic band origin. The band contour analysis[12] of the electronic band origin has been performed to identify the excitation selection rule and this was found to be type A. Thus, the excitation type for its $S_0 \rightarrow S_1$ electronic transition is A-A in C_2 symmetry and all the vibrational modes in the spectrum, except the ring puckering (ν_{61}) and ring flapping (ν_{59}) modes, belong to the totally symmetric mode (species A).

As shown in Table 2, a series of bands at 93.8, 189.0, and 282.7 cm^{-1} was assigned to the twisting mode of the

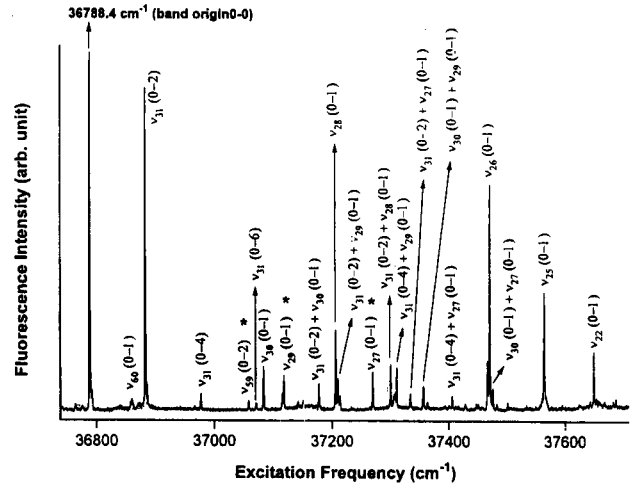

Figure 5. Jet-cooled laser-induced fluorescence excitation spectrum of tetralin in the 265-273 nm region. The bands, marked with *, have been reassigned.

Table 2. Observed S_1 transition frequencies (cm^{-1}) and assignments from the jet-cooled laser-induced fluorescence excitation spectrum of tetralin

ν (cm^{-1})	Displacement From origin (0_0^0)	Chowdhury *et al.*[a]	Assignment[b]
36788.4	0.0	0	0_0^0
36859.8	71.4	–	60_0^1
36882.2	93.8	95	31_0^2
36977.4	189.0	189	31_0^4
37058.6	270.2	270 (60_0^2 31_0^2)	59_0^2
37071.1	282.7	282	31_0^6
37083.7	295.3	295 (coupled mode)	30_0^1
37118.1	329.7	329 (coupled 59_0^1)	29_0^1
37178.1	389.7	390	31_0^2 30_0^1
37206.4	418.0	418	28_0^1
37211.0	422.6	422	31_0^2 29_0^1
37270.1	481.7	481 (31_0^4 30_0^1)	27_0^1
37300.1	511.7	511	31_0^2 28_0^1
37310.3	521.9	520	31_0^4 29_0^1
37356.7	568.3	–	31_0^2 27_0^1
37407.7	619.3	–	30_0^1 29_0^1
37466.0	677.6	–	31_0^4 27_0^1
37470.0	681.6	679	26_0^1
37501.5	713.1	–	30_0^1 27_0^1
37563.9	775.5	765	25_0^1
37649.6	861.2	–	22_0^1

[a] Reference 3. [b] Assignment notation $[\nu_i]_x^y$ ndicates a $x \rightarrow y$ transition for ν_i.

saturated six-membered ring. The band progression of this mode was very similar to that of 1,4-benzodioxan.[5] A couple of very weak ring puckering and ring flapping bands were observed at 71.4 and 270.2 cm^{-1}, respectively. These two vibrational modes belong to the non-totally symmetric species B. The band at 270 cm^{-1} had been assigned to a hot band ($60_0^2 31_0^2$) by Chwodhury, but it was reassigned in our study as a second overtone ring flapping mode (59_0^2) based on the assignment of 1,4-benzodioxan.[5] The band at 329 cm^{-1}, which had been assigned as a coupled double bond torsion, was reassigned as the fundamental mode of ring angle deformation. This is because this band is too intense to be observed as a symmetrically forbidden mode.

Ring Inversion Process of Tetralin in its S_0 State

The ring inversion process of cyclohexene has been extensively investigated by the spectroscopic and *ab initio* methods. Rivera-Gaines *et al.*[6(a)] have analyzed the gas phase far-infrared spectra of cyclohexene and used the data to define a two-dimensional potential energy surface in terms of the twisting and bending coordinates. This surface has a ring inversion barrier of 10.3 kcal/mol. Anet and coworkers[6(b)] have also examined the conformational changes of cyclohexene using the *ab initio* and MM3 methods. Their MM3 and *ab initio* calculations at moderate levels predicted an inversion barrier of 5.5-6.6 kcal/mol. Figure 6(a) compares the experimental potential energy profile with the calculated ones. The calculated potential profiles have

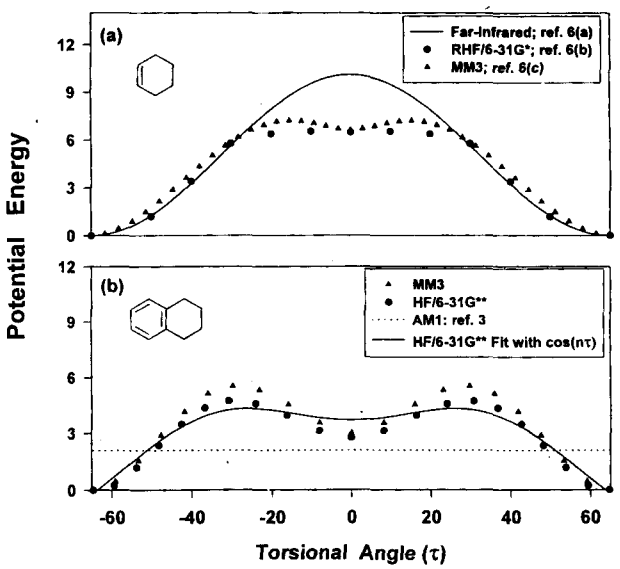

Figure 6. Potential energy profiles for ring inversion as a function of torsional angle (τ): (a) cyclohexene; (b) tetralin.

the narrow potential dips. In the case of cyclohexene the experimental barrier height, determined by far-infrared spectroscopy, is much higher than the values calculated from the *ab initio* and MM3 methods. In order to explain these discrepancies, Laane and Choo[6(c)] investigated the ring inversion of cyclohexene by treating this process as a hindered pseudorotation. They confirmed that the actual inversion barrier height is about 3-5 kcal/mol higher than the values calculated from the *ab initio* and MM3 methods.

The ring inversion process of tetralin is considered very similar with that of cyclohexene because the benzene ring of tetralin makes the ring rigid like the olefinic double bond of cyclohexene. High-resolution gas phase far-infrared spectroscopy can be utilized to determine an experimental potential energy surface in terms of the twisting and bending coordinates. Unfortunately, the boiling point of tetralin is too high (b.p. 207 °C) to obtain a gas phase far-infrared spectrum.

Chowdhury and co-workers performed the conformational analysis of tetralin using AM1 calculations, and they have determined the inversion barrier to be 2.1 kcal/mol.[3] This barrier height is, however, too low even though we consider the fact that the rigidity of the benzene ring reduces the potential barrier to a certain extent. They also recognized this problem, and mentioned that the *ab initio* calculations should be done to determine an accurate inversion barrier for tetralin. In order to determine a more reasonable barrier height, we have carried out the MM3 and *ab initio* calculations for the ring inversion process of tetralin. Figure 6(b) shows the HF/6-31G** and MM3 potential energy profiles of tetralin as a function of the CH_2-CH_2-CH_2-CH_2 torsional angle of the saturated six-membered ring. The calculation was initiated with the coordinates at the conformational minimum (*i.e.*, twisted form: torsional angle=64.8°). The torsional angle was then incrementally decreased to 0°, and the energy and structure were calculated at each point. Both MM3 and *ab initio* profiles of tetralin have deeper potential dips than those of cyclohexene and the shapes of po-

tential profiles calculated from the MM3 and HF/6-31G** methods are very similar. Whether a potential dip is actually present is difficult to ascertain because the experimental potential energy function has not been determined for the inversion of tetralin. The potential dip, for the inversion of cyclohexene, was not certain either because the spectroscopically observed data only extended about 3.0 kcal/mol above the potential minima and the potential barrier was determined from the smooth extrapolation of potential energy surface.[6(c)] In order to understand the origin of the physical forces to cause the narrow potential dip, we have analyzed the energy components of total steric energy calculated by MM3. This analysis indicated that the total steric energy is exclusively affected by the torsional energy components. As the molecule twists from the bending conformation, the angle strain decreases as the C-C-C angle of the six-membered ring are reduced to tetrahedral values. However, the torsional strain about the CH_2-CH_2 bonds was expected to be increased and the decrease of angle strain was more than off-set by the torsional strain. Thus, the total steric energy was slightly increased up to τ=30°. On the other hand, the total steric energy was decreased over this range because both angle strain and torsional strain were expected to be decreased together over τ=30°. In order to estimate a reasonable barrier height, we have used a potential function of the form[13]

$$V_n = \frac{1}{2}\sum_n V_n(1+\cos n\tau) \quad (1)$$

where V_n represents an n-fold barrier. The best fit with the calculated HF/6-31G** (Figure 6(b)) is obtained with V_2=6.5 kcal/mol, V_4=−2.3 kcal/mol, and V_6=−0.4 kcal/mol, and a barrier in the 3.7-4.3 kcal/mol range. This range might be lower than an experimental potential barrier but it is much higher than the previously reported AM1 value of 2.1 kcal/mol.[3]

Conclusion

In this work we observed the infrared and Raman spectra of tetralin as well as the fluorescence excitation spectrum in a helium supersonic nozzle beam. All the vibrational modes in the S_0 state have been assigned based on Raman depolarization ratios, group frequency considerations and the assignments for related compounds. The *ab initio* calculations at the HF/6-31G** basis set level, with a single scaling factor of 0.89, were found to reproduce the S_0 vibrational frequencies very well. Sometimes the vibrational frequencies calculated from the *ab initio* methods made it possible to assign the ambiguous spectral bands.

The low frequency vibrational modes of tetralin in the S_1 state were also assigned from the fluorescence excitation spectrum. Our assignments basically agree with those of Chowdhury but a couple of fundamental bands and four hot bands were observed in our spectrum for the first time. In addition, the fundamental modes, for ring flapping and angle deformation, were reassigned based on the selection rules for its $S_0 \rightarrow S_1$ electron transition and the previous assignments of 1,4-benzodioxan.

The ring inversion process of tetralin between two twisted conformations has been reexamined using the *ab initio* and MM3 calculations. The inversion barrier calculated from these methods is in the 3.7-4.3 kcal/mol range and this range is much higher than the previously reported AM1 value of 2.1 kcal/mol. The lower inversion barrier height of tetralin, compared to cyclohexene (8.4-12.1 kcal/mol), is caused by the rigidity of the benzene ring. It is expected, however, that the experimental barrier height of tetralin is slightly higher than the calculated range of 3.7-4.3 kcal/mol based on the results of the far-infrared study of cyclohexene.

Acknowledgment. This paper was supported by NON DIRECTED RESEARCH FUND, Korea Research Foundation, 1996.

References

1. (a) Juaristi, E. *Conformational Behavior of Six-Membered Rings*; Jusristi, E. Ed.; VCH; New York, 1995; pp 1-203. (b) Case, D. A. *Conformational Analysis of Medium-Sized Heterocycles*; Glass, R. S. Ed.; VCH: New York, 1988; pp 65-210. (c) Laane, J. *Annu. Rev. Phys. Chem.* **1994**, *45*, 179.
2. (a) Hollas, J. M. *Large Amplitude Vibrations in Electronic Spectra in Supersonic Jets*; Fausto, R. Ed.; NATO ASI Series; Kluer Academic Publisher; Dordrecht, 1996; pp 311-350. (b) Hassan, K. H.; Hollas, J. M. *J. Mol. Spectrosc.* **1991**, *147*, 100. (c) Zgierski, M. Z.; Zerbetto, F.; Shin, Y-D.; Lim, E. C. *J. Chem. Phys.* **1992**, *96*, 7229.
3. Guchhait, N.; Chakraborty, T.; Majumdar, D.; Chowdhury, M. *J. Phys. Chem.* **1994**, *98*, 9227.
4. Lin-Vien, D.; Colthup, W. G.; Fately, W. G.; Grasselli, J. G. *The Handbook of Infrared and Raman Characteristic Frequencies of Organic Molecules*; Academic Press: San Diego, 1991; pp 1-94.
5. (a) Gordon, R. D.; Hollas, J. M. *J. Chem. Phys.* **1993**, *99*, 3380. (b) Gordon, R. D.; Hollas, J. M. *J. Mol. Struct.* **1993**, *293*, 193.
6. (a) Rivera-Gaines, V. E.; Leibowitz, S. J.; Laane, J. *J. Am. Chem. Soc.* **1991**, *113*, 9735. (b) Anet, F. A. L.; Freedberg, D. I.; Storer, J. W.; Houk, K. N. *J. Am. Chem. Soc.* **1992**, *114*, 10969. (c) Laane, J.; Choo, J. *J. Am. Chem. Soc.* **1994**, *116*, 3889.
7. Choo, J.; Kim, T. S.; Choi, Y. S. *Bull. Korean Chem. Soc.* **1996**, *17*, 461.
8. Frisch, M. J.; Trucks, G. W.; Head-Gordon, M.; Gill, P. M. W.; Wong, M. W.; Foresman, J. B.; Johnson, B. G.; Schlegel, H. B.; Robb, M. A.; Replogle, E. S.; Gomperts, R.; Andres, J. L.; Raghavachari, K.; Binkley, J. S.; Gonzalez, C.; Martin, R. L.; Fox, D. J.; Defrees, D. J.; Baker, J.; Stewart, J. J. P.; Pople, J. A. *GAUSSIAN 94*; Gaussian, Inc., Pittsburgh PA, 1994.
9. (a) Allinger, N. L.; Yuh, Y. H.; Lii, J. H. *J. Am. Chem. Soc.* **1989**, *111*, 8551. (b) Lii, J. H.; Allinger, N. L. *J. Am. Chem. Soc.* **1989**, *111*, 8556. (c) Lii, J. H.; Allinger, N. L. *J. Am. Chem. Soc.* **1989**, *111*, 8576.
10. Pulay, P.; Meyer, W. *Mol. Phys.* **1974**, *27*, 473.
11. (a) Pulay, P. *J. Mol. Struct.* **1995**, *347*, 293. (b) Rauhut, G.; Pulay, P. *J. Phys. Chem.* **1995**, *99*, 3093. (c) Scott, A.; Radom, L. *J. Phys. Chem.* **1996**, *100*, 16502.
12. (a) Van der Veken, B. J. *Vibrational Spectra and Structure, Vol. 15*; Durig, J. R. Ed.; Dekker; New York,

1986; pp 313-400. (b) Choo, J.; Lee, K-H.; Laane, J. *J. Mol. Struct.* **1996**, *376*, 255.
13. (a) Lewis, J. D.; Malloy, T. B. Jr.; Chao, T. H.; Laane, J. *J. Mol. Struct.* **1972**, *12*, 427. (b) Choo, J.; Laane, J. *J. Chem. Phys.* **1994**, *101*, 2772.

Interaction of Oxygen and CH_4 with Molybdenum Oxide Catalysts

C. M. Kim

Department of Chemistry, Kyungpook National University, Taegu 702-701, Korea
Received June 16, 1997

The Near-Edge X-ray Absorption Fine Structure (NEXAFS) technique and Differential Scanning Calorimetry (DSC) were utilized to investigate the reaction of CH_4 and O_2 on the MoO_3/SiO_2 catalyst. The NEXAFS results showed that the stoichiometry of the molybdenum oxide catalyst supported on silica was MoO_3. MoO_3 was reduced to MoO_2 when the catalyst was exposed to CH_4 at 773 K. NEXAFS results confirm that lattice oxygen is directly related to the process of CH_4 oxidation which takes place on the surface of MoO_3/SiO_2 catalysts. DSC results show that the structure of MoO_3 changes around 573 K and this structural change seems to improve the migration of oxygen in the lattice.

Introduction

The MoO_3/SiO_2 catalyst is used for the partial oxidation of CH_4 to HCHO and CH_3OH.[1-3] Catalytic oxidation of methane to produce valuable hydrocarbons has been extensively studied.[4,5] However, a lot of controversial results have been reported about the active species and reaction intermediates which are responsible for the partial oxidation of methane on the catalyst surface. One of the questions about catalytic oxidation of methane over MoO_3 is the role of lattice oxygen during the oxidation process. It has not been clearly determined whether lattice oxygen is directly related to the oxidation process. Isotopic labelling technique has been utilized to probe the origin of the oxygen species incorporated into reaction products.[6] However, a definitive proof could not be obtained because of the isotopic exchange between the reaction products and labelled oxygen. In this paper, we will propose that lattice oxygen of MoO_3 takes part in the oxidation process of CH_4.

We utilized the Near-Edge X-ray Absorption Fine Structure (NEXAFS) technique and Differential Scanning Calorimetry (DSC) to investigate the MoO_3/SiO_2 catalyst. NEXAFS is a very powerful technique to investigate metal oxide surfaces. Among the capabilities of NEXAFS are: determination of chemical composition, the ability to detect the presence of specific bonds and determination of bond lengths of molecules, and the derivation of the precise orientation of molecules on surfaces or in solids.[7] In the NEXAFS experiment, we detect both Auger electrons and fluorescence emission caused by X-ray absorption. Because we record both electron yield and fluorescence yield, the effect of surface charging can be minimized. Surface charging sometimes causes serious problems when the insulating material is analyzed using electron spectroscopy such as X-ray photoelectron spectroscopy. We will show that NEXAFS is an ideal technique for the study of insulating metal oxide catalysts.

Experimental Methods

The MoO_3/SiO_2 catalysts were prepared by conventional pore volume impregnation technique using aqueous solution of high purity $(NH_4)_6Mo_7O_{24}\cdot 4H_2O$ and silica gel. The surface area of silica gel was 300 m^2/g and the pore volume was 1.15 cm^3/g. After impregnation, the catalysts were dried at 120 °C for 10 hours and then calcined at 550 °C for 6 hours. Figure 1 shows the XRD profile of the MoO_3/SiO_2 catalyst prepared by this method. It clearly shows the orthorhombic structure when MoO_3 loading was 15% by weight. This implies that MoO_3 forms 3 dimensional particles on SiO_2. The particle size was estimated to be 330 Å based on

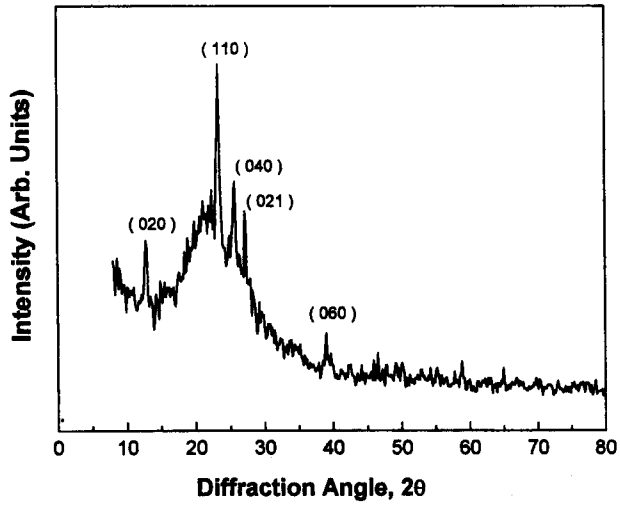

Figure 1. XRD pattern of MoO_3/SiO_2. MoO_3 loading on SiO_2 is 15% by weight.